Accuracy of density functionals for molecular electronics: The Anderson junction

Zhen-Fei Liu, Justin P. Bergfield, and Kieron Burke
Department of Chemistry and Department of Physics, University of California, Irvine, California 92697, USA

Charles A. Stafford
Department of Physics, University of Arizona, 1118 East Fourth Street, Tucson, Arizona 85721, USA
(Received 5 January 2012; revised manuscript received 21 March 2012; published 9 April 2012)

The exact ground-state exchange-correlation functional of Kohn-Sham density functional theory yields the exact transmission through an Anderson junction at zero bias and temperature. The exact impurity charge susceptibility is used to construct the exact exchange-correlation potential. We analyze the successes and limitations of various types of approximations, including smooth and discontinuous functionals of the occupation, as well as symmetry-broken approaches.

DOI: 10.1103/PhysRevB.85.155117 PACS number(s): 71.15.Mb, 31.15.E−, 73.23.−b, 31.10.+z

I. INTRODUCTION

Since the pioneering experiments of Reed and Tour on dithiolated benzene,[1] there has been tremendous progress in the ability to both create and characterize[2] organic molecular junctions. But accurate simulation of these devices remains a challenge, both theoretically and computationally.[3] The essential physics has been well understood since the groundbreaking work of Landauer and Büttiker[4,5] in the context of mesoscopic devices, including both Coulomb blockade and Kondo effects.[6,7] Calculations with simple model Hamiltonians demonstrate such effects at a qualitative level.[8] On the other hand, organic molecules connected to metal leads[9] require hundreds of atoms and thousands of basis functions for a sufficiently accurate calculation of their total energy, geometry, and single-particle states. Such conditions are routine for modern density functional theory (DFT) calculations,[10] but the ability of present functional approximations to predict accurate currents remains an open question.[11]

The standard DFT method for calculating current through such a device is to perform a ground-state Kohn-Sham (KS) DFT calculation[12] on a system upon which a difference between the chemical potentials of the left and right leads has been imposed (the applied bias) and calculate the transmission through the KS potential using the Landauer-Büttiker formula. But there is nothing in the basic theorems of DFT that directly implies that such a calculation would yield the correct current, even if the exact ground-state functional were used.

The limit of weak bias is more easily analyzed than the general case because the Kubo linear response formalism applies.[13,14] In that case one finds that, in principle, there are exchange-correlation (XC) corrections to the current in the standard approach,[15] but little is known about their magnitude.[16,17] Even without these corrections, one can ask if the standard approximations used in most ground-state DFT calculations (i.e., generalized gradient approximations[18] and hybrids of these with Hartree-Fock exchange[19,20]) are sufficiently accurate for transport purposes. The answer appears definitively no. Because of self-interaction errors, such approximations are well known[21] to produce potentials with incorrectly positioned KS eigenvalues, both occupied and unoccupied. These errors become severe when the molecule is only weakly coupled to the leads.[22,23] Calculated transmission can be too large by several orders of magnitude due to this incorrect positioning of the levels. Recent calculations[24] using beyond-DFT techniques to correctly position the levels show greatly improved agreement with experiment.

But this progress returns us to the earlier concern: Even with an exact ground-state XC functional, are there XC corrections to the Landauer-Büttiker result? The answer appears to be yes in general,[15] but in a previous work[25] we argued that, under a broad range of conditions applicable to typical experiments, such corrections can vanish. This result was shown by exact calculations on an impurity model (Anderson model) employing the exact XC functional. Similar results were achieved independently by other groups at about the same time.[26,27] In the present work, we analyze different approximate treatments, applied to the Anderson junction, and calculate their errors. The implications for DFT calculations of transport in general are discussed.

The Anderson model[28] is a single interacting site (C) connected to two noninteracting electrodes (L,R). The Hamiltonian of the system is $\mathcal{H} = \mathcal{H}_{\rm C} + \mathcal{H}_{\rm T} + \mathcal{H}_{\rm L,R}$. Each lead is represented by a noninteracting Fermi gas, $\mathcal{H}_{\rm L,R} = \sum_{k\sigma\in L,R} \varepsilon_{k\sigma}\hat{n}_\sigma$, with chemical potential μ, and the central interacting site is $\mathcal{H}_{\rm C} = \varepsilon(\hat{n}_\uparrow + \hat{n}_\downarrow) + U\hat{n}_\uparrow\hat{n}_\downarrow$, where $\hat{n}_\sigma = d_\sigma^\dagger d_\sigma$ is the number operator for spin σ and U is the charging energy representing on-site interaction. $\mathcal{H}_{\rm T}$ is the tunneling between leads and the central site. The tunneling width Γ is a constant in the broad-band limit. A schematic is shown in Fig. 1. Real molecules can be mapped onto the Anderson model.[29,30]

In a previous work,[25] we calculated the exact relation between occupancy on the central site and on-site energy ε for an Anderson junction, using the Bethe ansatz (BA).[31] We showed that exact KS DFT yields the exact transport at zero temperature and in the linear response regime, although the KS spectral function differs from the exact one away from the Fermi energy. This is because the Anderson junction has only one site and transmission is a function of occupation number due to the Friedel-Langreth sum rule.[32,33] The connection to transport was pointed out in Refs. 24 and 34. Thus, for this simple model, all failures of approximate XC calculations of transmission can be attributed to failures to reproduce the exact occupation number; i.e., there are *no* XC corrections to the standard practice of applying KS DFT to the ground state

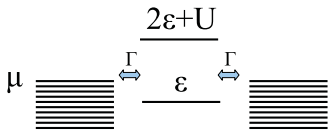

FIG. 1. (Color online) A cartoon of the Anderson model. The model consists of two featureless leads and a central region with on-site interaction U. Γ is the tunneling width. Two many-body levels of the central region are shown.

and finding transmission through the single-particle potential. On the other hand, the standard approximations in use in DFT calculations of transport have a variety of shortcomings. The most prominent one, as we shall see, is the lack of a discontinuity in the XC potential with particle number.[35]

II. PARAMETRIZATION OF XC POTENTIAL

Before studying approximations, we refine our previous numerical fit of BA results, using analytic results from many-body theory. We reintroduce[28] reduced variables $y = \Gamma/U$, which measures the ratio of lead coupling to the on-site Coulomb repulsion, and $x = (\mu - \epsilon)/U$, which is the difference between the leads' chemical potential and the on-site level energy, in units of U. For $x < 0$, the central site is above the chemical potential; at $x = 0$ they match.

The occupation in the KS system is given by a self-consistent solution of the KS equation for occupation:

$$\langle n_c \rangle = 1 + \frac{2}{\pi} \arctan\left(\frac{\mu - \varepsilon_s(\langle n_c \rangle)}{\Gamma}\right), \tag{1}$$

where the KS level is written as

$$\varepsilon_s(\langle n_c \rangle) = \varepsilon + \frac{U}{2}\langle n_c \rangle + \varepsilon_{xc}(\langle n_c \rangle), \tag{2}$$

with the second term being the Hartree contribution and the third being the XC contribution (in fact, only correlation, as exchange is zero for this model), which is a function of the occupation. Considered in reverse, this is a *definition* of the exact ε_{xc}, if the occupation is known, as it is from the BA solution. The KS transmission is then

$$T(E)_{E=\mu} = \sin^2\left(\frac{\pi}{2}\langle n_c \rangle\right) \tag{3}$$

and matches the *true* transmission in the many-body system by virtue of the sum rule. The exact ground-state functional yields the exact transmission, including the Kondo plateau at zero temperature and weak bias.[25,36]

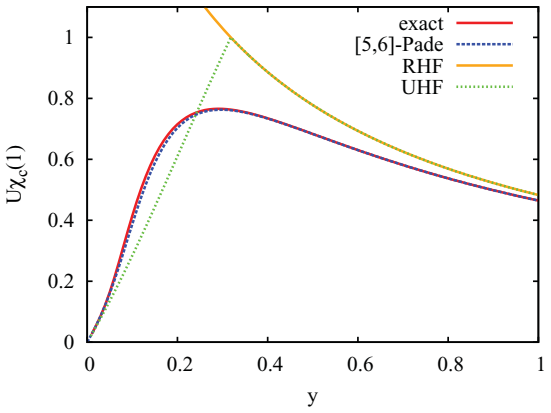

FIG. 2. (Color online) Dimensionless susceptibility $\tilde{\chi}_c = U\chi_c(1)$ as a function of $y = \Gamma/U$ for the Anderson junction [exact, [5, 6] Padé fit (see text), RHF, and UHF].

As shown in Ref. 25, the XC potential can be very accurately parametrized with the form

$$\frac{\varepsilon_{xc}}{U} = \frac{\alpha}{2}\left[1 - \langle n_c \rangle - \frac{2}{\pi}\tan^{-1}\left(\frac{1 - \langle n_c \rangle}{\sigma}\right)\right]. \tag{4}$$

The $\tan^{-1}$ term jumps by π as $\langle n_c \rangle$ passes through 1, leading to discontinuous behavior with occupation. Thus σ determines the width of this region, while α determines its strength. Both σ and α are functions of $y = \Gamma/U$ and were extracted numerically by fitting to the exact solution and were roughly fit by simple Padé approximations there.

However, we can greatly improve the fit of σ. A central object in the Anderson junction is the charge susceptibility, $\chi_c(\langle n_c \rangle) = d\langle n_c \rangle/d\mu$. At half-filling, this is known analytically:[37,38]

$$\tilde{\chi}_c = \frac{1}{\pi}\sqrt{\frac{2}{y}}\int_{-\infty}^{\infty} dt\, \frac{e^{-\pi y t^2/2}}{1 + [(2y)^{-1} + t]^2}, \tag{5}$$

where $\tilde{\chi}_c = U\chi_c(1)$ is dimensionless and is plotted in Fig. 2. This curve can be readily fit to a [5, 6] Padé form:

$$\tilde{\chi}_c^{\rm mod}(y) = \sum_{k=1}^{5} a_k y^k \Big/ \sum_{k=0}^{6} b_k y^k, \tag{6}$$

whose 11 independent coefficients are chosen to recover the Taylor expansion around $y = 0$ (strongly correlated limit)[39] exactly to 5 orders and around $y \to \infty$ to 6 orders and are given in Table I. The weak-correlation limit can also be extracted via the Yosida-Yamada perturbative approach.[40–42] The quantity

TABLE I. Coefficients in the [5, 6] Padé approximation [Eq. (6)].

k	a_k	b_k
0		$\pi^3(\pi^6 + 6\pi^4 - 225\pi^2 + 675)$
1	$8\pi^2$	$-12\pi^2(\pi^6 + 54\pi^4 - 945\pi^2 + 3105)$
2	$-576\pi(8\pi^4 - 120\pi^2 + 405)$	$12\pi(\pi^8 - 30\pi^6 + 555\pi^4 - 6525\pi^2 + 29700)$
3	$64(\pi^8 - 36\pi^6 + 153\pi^4 + 135\pi^2 + 8910)$	$96(\pi^8 - 80\pi^6 + 975\pi^4 - 2925\pi^2 + 1350)$
4	$256\pi(4\pi^6 - 204\pi^4 + 1530\pi^2 + 945)$	$48\pi(\pi^8 - 30\pi^6 - 225\pi^4 + 3375\pi^2 + 8100)$
5	$128\pi^2(\pi^6 - 42\pi^4 + 315\pi^2 + 135)$	$576\pi^2(\pi^6 - 50\pi^4 + 375\pi^2 + 225)$
6		$\pi a_5/2$

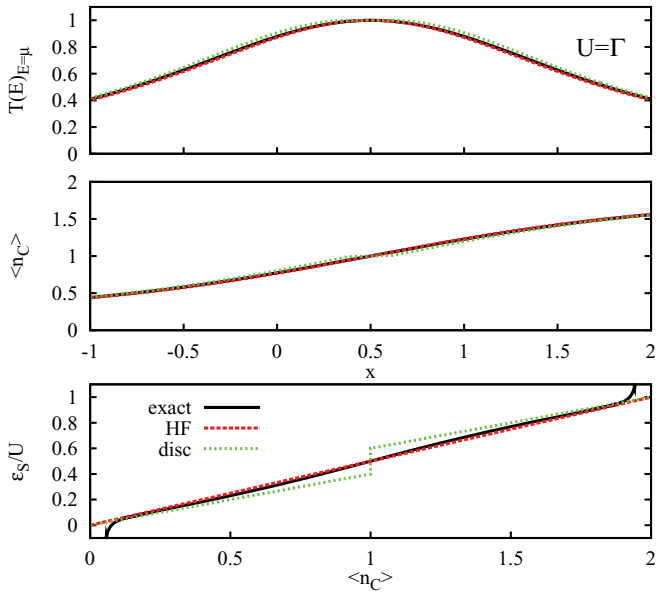

FIG. 3. (Color online) (top) Transmission as a function of $x = (\mu - \epsilon)/U$, (middle) occupation as a function of x, and (bottom) KS potential as a function of occupation. Results are shown for Bethe ansatz or exact KS DFT (exact), Hatree-Fock (HF), and discontinuous approximation [disc, Eq. (10)]. $U = \Gamma$ in all cases.

$\tilde{\chi}_c$ has the physical meaning of the slope at the particle-hole symmetry point in the $\langle n_c \rangle$ vs $(\mu - \epsilon)/U$ curve (see Figs. 3 and 4). It has a maximum at about $y = 0.291$, and as y varies from ∞ (weakly correlated limit) to 0 (strongly correlated limit), the slope at the symmetric point increases at first. Beyond the maximum value, the slope decreases, and the Coulomb blockade plateau gradually develops.

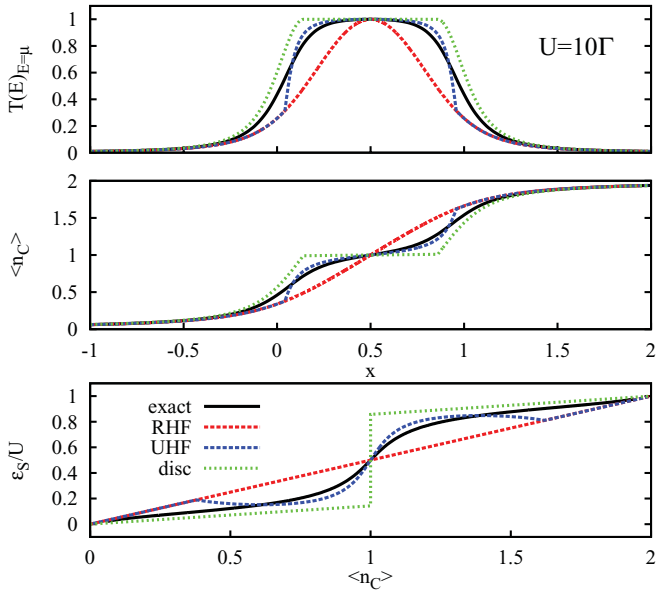

FIG. 4. (Color online) (top) Transmission as a function of $x = (\mu - \epsilon)/U$, (middle) occupation as a function of x, and (bottom) KS potential as a function of occupation. Results are shown for Bethe ansatz or exact KS DFT (exact), RHF, UHF, and discontinuous approximation [disc, Eq. (10)]. $U = 10\Gamma$ in all cases.

By taking derivatives on both sides of Eq. (4), the two coefficients α and σ are constrained by $\tilde{\chi}_c$:

$$\sigma = \frac{2\alpha}{\pi\,(2/\tilde{\chi}_c - y\pi + \alpha - 1)}. \tag{7}$$

Retaining the simple form of Ref. 25, a [0,1] Padé, $\alpha = 1/(1 + 5.68y)$, we determine σ from the Padé fit to the susceptibility and Eq. (7). This yields highly accurate occupations, KS potentials, and transmissions, including the Kondo plateau. It agrees very well with the numerical fit to the BA results of Ref. 25 and matches more closely than the simpler analytic fit used there.

III. PERFORMANCE OF APPROXIMATIONS

We now move on to the central topic of this work, which is the accuracy of approximate functional treatments. In such treatments, ε_{xc} is approximated as a function of $\langle n_c \rangle$ in Eq. (2), and the resulting Eq. (1) is solved self-consistently for $\langle n_c \rangle$. The simplest such approximation is to simply set $\varepsilon_{xc} = 0$, i.e., the Hartree-Fock (HF) method, and should be accurate when correlation is weak. In Fig. 3, we plot several quantities for $U = \Gamma$, both exactly and in HF, showing that HF is very accurate here. We find[28]

$$\tilde{\chi}_c^{\rm HF} = \frac{2}{1 + y\pi}, \tag{8}$$

which is correct to leading order in y^{-1}:

$$\tilde{\chi}_c \to 2/(\pi y) - 2/(\pi y)^2 + 2\gamma/(\pi y)^3 + \cdots \qquad y \to \infty, \tag{9}$$

where $\gamma = 3 - \pi^2/4$ exactly but $\gamma = 1$ in HF. Thus we regard $U \lesssim \Gamma$ as the weakly correlated regime. On the other hand, in Fig. 4, we show the same plots for $U = 10\,\Gamma$. Now, in the exact occupation, the slope near $x = 0.5$ is much weaker, leading to a transmission plateau (the Kondo plateau) for $0 \leqslant x \leqslant 1$. The plateau effect is missed entirely by HF because of the too smooth dependence (in fact, linear) of its KS level on occupation (see bottom panel). Note that at temperatures equal to or above the Kondo temperature, the Kondo effect is destroyed, and the central plateau in transmission is replaced by two Hubbard peaks around $x = 0$ and 1. Then the behavior of the HF curve is exactly as qualitatively predicted in Ref. 15, smearing out the two sharp features into one peak midway between them. This is because the KS level shifts linearly with occupation in HF, instead of more suddenly with occupation in the exact solution. More generally, all smooth density functionals, such as the local density approximation[12] and the generalized gradient approximation,[18] suffer from the same qualitative failure and so would produce incorrect peaks centered at $x = 0.5$. All these errors arise from the approximations to the functional; the exact ground-state functional reproduces the exact occupation by construction and so yields the exact transmission.

There have thus been several suggestions to incorporate the discontinuous behavior with occupation into approximations in transport calculations. At the practical level, Toher *et al.*[22] showed in a model calculation how self-interaction corrections would greatly suppress zero-bias conductance in local density approximation calculations for molecules weakly coupled to leads. More recently, the Bethe ansatz

local density approximation (BALDA),[43] developed for the one-dimensional Hubbard model, was used to investigate the transport properties of the Anderson model;[44] a smoothing of the derivative discontinuity was also introduced,[44] but with a different functional form than Eq. (4). For simple models, all of these can be considered as LDA+U-like. The methodology of LDA+U[45] has become increasingly popular in recent years, especially for those focused on moderately correlated systems such as transition metal oxides, for which LDA and generalized gradient approximation (GGA) often have zero KS band gap. In some fashion, a Hubbard U is added to some orbitals of a DFT Hamiltonian. Sometimes U is regarded as an empirical parameter, while others have found self-consistent prescriptions. In any event, despite not fitting in the strict DFT framework, it is a method borne of practical necessity for many situations.[46]

To gain a qualitative understanding of the effects of such models, we define a very simple XC potential that has a discontinuity. To do this, we simply take the Hartree form, symmetrize it around the half-filled point, and replace U by a screened $\tilde{U}$. We find that a simple fit $\tilde{U} = U/(1 + 0.25/y)$ works well. $\tilde{U}$ being different from U and particle-hole symmetry guarantee an explicit derivative discontinuity of ε_s with respect to occupation number. This yields

$$\varepsilon_s[n] = \frac{1}{2}\tilde{U}n\theta(1-n) + \left[U + \frac{1}{2}\tilde{U}(n-2)\right]\theta(n-1), \quad (10)$$

where $\theta(x)$ is the Heaviside θ function and, for simplicity, n is just $\langle n_C \rangle$.

While this model does contain a discontinuity and yields the exact result as $y \to 0$, curing the worst defects of HF, it misses entirely the finite slope of the KS potential at half-filling for finite U, which is determined by the susceptibility. The explicit derivative discontinuity is exact in the strongly correlated limit with infinite U/Γ but should be "rounded" in finite U/Γ (Refs. 25 and 49) or in finite temperature.[27] To see this for finite (but very large) U/Γ, in Fig. 5, we show similar results as in Figs. 3 and 4, but with $U = 100\Gamma$, and we only show the region around $\langle n_C \rangle = 1$ at $x = 0$, where the rounded derivative discontinuity occurs. The transmission is accurate both for weak and strong correlations but is not so everywhere in between. In particular, it is overestimated for $\langle n_C \rangle$ just above 0 (and just below 1) for $U = 10\Gamma$ because of this lack of a finite slope. This is where we expect the greatest errors in such models, but the region of inaccuracy (on the scale of x) shrinks as $U/\Gamma \to \infty$.

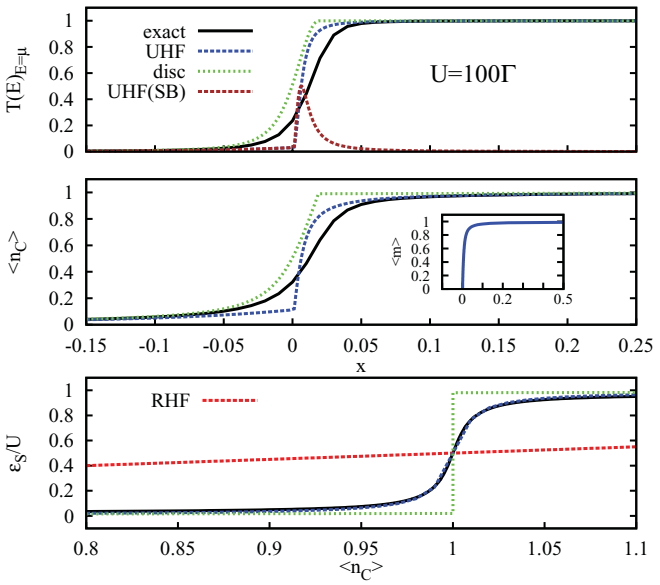

FIG. 5. (Color online) (top) Transmission as a function of $x = (\mu - \epsilon)/U$, (middle) occupation as a function of x, and (bottom) KS potential as a function of occupation. Results are shown for Bethe ansatz or exact KS DFT (exact), unrestricted Hartree-Fock (UHF), and discontinuous approximation [disc, Eq. (10)]. Also shown in the top panel are UHF results for transmission using (incorrect) spin densities [UHF(SB), with symmetry breaking], and $\langle m \rangle = \langle n_\uparrow \rangle - \langle n_\downarrow \rangle$ for UHF as a function of x is shown as an inset in the middle panel. $U = 100\Gamma$ in all cases, and only the region near $\langle n_C \rangle = 1$ and $x = 0$ is shown.

IV. BREAKING SPIN SYMMETRY

Finally, we discuss a different class of approximations. A well-known (and much debated) technique for mimicking strong correlation is to allow a mean-field calculation to break symmetries that are preserved in the exact calculation. Perhaps the most celebrated prototype of such a calculation is for HF applied to an H_2 molecule with a large bond distance. At a crucial value of the bond distance (called the Coulson-Fischer point), an *unrestricted* calculation, i.e., one that allows a difference in spin occupations, yields a lower energy than the restricted one. This remains the case for all larger separations, and the unrestricted solution correctly yields the sum of atomic energies as $R \to \infty$, whereas the restricted Hartree-Fock (RHF) solution dissociates to unpolarized H atoms with the wrong energies. This is the celebrated symmetry dilemma: with a mean-field approximation, for large separations, one can either get the right symmetry (RHF) or the right energy [unrestricted Hartree-Fock (UHF) solution], but not both. The same issues arise in approximate DFT treatments of this problem.[47] Of course, the exact functional manages to get the correct energy with the correct symmetry, and there have been many attempts to reproduce this with various more sophisticated approximations. But a more pragmatic approach is to accept the results as they are, interpreting the good energetics as the result of applying the approximate functional to a frozen fluctuation of the system. The true ground-state wave function fluctuates between configurations with one spin and then the other (left and right localized for stretched H_2), and the true ground-state density has unbroken symmetry. But the approximate functionals give most accurate energies when applied to the frozen fluctuations. Thus, one can interpret both the *total* density and energy as being accurate from such a calculation, but not the individual spin densities. In fact, an alternative approach is to interpret another variable, such as the on-top pair density, as being accurately approximated in such treatments.[47]

We apply the same reasoning to the Anderson junction, just as was done by Anderson when creating the model we are using.[28] The symmetries are different, but the principle is the same. We allow the mean-field calculation to break spin symmetry if this leads to lower energy on the central site, with

spin equations

$$\langle n_\uparrow\rangle = \frac{1}{2} + \frac{1}{\pi}\arctan\left(\frac{\mu - \varepsilon - U\langle n_\downarrow\rangle - \varepsilon_{\rm xc}(\langle n_\uparrow\rangle,\langle n_\downarrow\rangle)}{\Gamma}\right) \tag{11}$$

and the reverse for $\langle n_\downarrow\rangle$ and $\langle n_{\rm c}\rangle = \langle n_\uparrow\rangle + \langle n_\downarrow\rangle$. Again, the simplest calculation is UHF, where $\varepsilon_{\rm xc} = 0$. The solutions are identical to those found in the original problem by Anderson.[28] For $y > 1/\pi$, i.e., $U < \pi\Gamma$, there is no spontaneous symmetry breaking, and UHF = RHF. But beyond that critical value, the spin-density difference becomes finite, and the unrestricted solution differs. Define the density difference as $\langle m\rangle = \langle n_\uparrow\rangle - \langle n_\downarrow\rangle$ in UHF, which satisfies

$$\tan\left(\frac{\pi}{2}\langle m\rangle\right) = \frac{\langle m\rangle}{2y}. \tag{12}$$

This equation is valid for $\langle n_{\rm c}\rangle = 1$, and similar relations can be derived for other $\langle n_{\rm c}\rangle$. For $y > 1/\pi$, $\langle m\rangle = 0$, but otherwise, a solution with finite $\langle m\rangle$ exists. In all cases, we take only the total density from the UHF calculation, and we know the true $\langle m\rangle = 0$ always. In particular, as $y \to 0$ (strong correlation), $\tilde{\chi}_{\rm c} \to 0$ with the correct linear term:

$$\tilde{\chi}_{\rm c} \to (8/\pi)y + (96\gamma/\pi^2)y^2 + \cdots \qquad y \to 0, \tag{13}$$

where $\gamma = 1$ in the exact solution but $\gamma = 1/3$ in UHF. So UHF recovers the leading term. The green curve in Fig. 2 shows the UHF value of $\tilde{\chi}_{\rm c}$, demonstrating both its accuracy for both strongly and weakly correlated systems and the discontinuous change at $1/\pi$.

Even beyond the Coulson-Fisher point of $1/\pi$, the symmetry breaking only occurs for $0 \leqslant \langle m\rangle \leqslant 1$; i.e., outside this region, the UHF solution is that of RHF, as can be seen in the inset in the middle panel in Fig. 5. But the density is very accurately given by UHF (considering the scale of horizontal axis), and the KS potential develops the correct derivative discontinuity as $y \to 0$.

To demonstrate this accuracy, we plot the corresponding transmissions in Figs. 4 and 5, using Eq. (3). Figures 4 and 5 show how the transmission using $\langle n_{\rm c}\rangle$ from UHF is almost exact (considering the scale of horizontal axis). To demonstrate the error in ignoring the fact that the UHF produces incorrect spin densities, we also plot the transmission through such a solution, which is completely wrong (see dark red curve in the top panel of Fig. 5; only one peak is present because only the region near $x = 0$ and $\langle n_{\rm c}\rangle = 1$ is shown there). Our results are consistent with those of Ref. 28, justifying the use of the broken-symmetry solution to deal with strong correlation.

V. CONCLUSIONS

To summarize, we have studied approximate treatments of the zero-temperature weak-bias conductance of the Anderson junction. RHF and approximate DFT treatments work well for weak correlation but fail for moderate and strong correlation because of the smooth dependence of their KS potentials on occupation numbers. Imposing an explicit discontinuity consistent with particle-hole symmetry can yield a discontinuity with occupation which guarantees correct behavior in the strong-correlation limit. This also greatly improves results for moderate correlation but still contains errors. Finally, simple symmetry breaking in UHF produces remarkably accurate conductances, once the transmission is calculated *as if* the symmetry had *not* been broken.

ACKNOWLEDGMENTS

K.B. acknowledges support from the Department of Energy under Award No. DE-FG02-08ER46496. C.A.S. acknowledges support from the Department of Energy under Award No. DE-SC0006699.

[1] M. A. Reed, C. Zhou, C. J. Muller, T. P. Burgin, and J. M. Tour, Science **278**, 252 (1997).
[2] *Introducing Molecular Electronics*, edited by G. Cuniberti, G. Fagas, and K. Richter (Springer, Berlin, 2005).
[3] A. Nitzan and M. A. Ratner, Science **300**, 1384 (2003).
[4] R. Landauer, IBM J. Res. Dev. **1**, 223 (1957).
[5] M. Büttiker, Phys. Rev. Lett. **57**, 1761 (1986).
[6] Y. Meir, N. S. Wingreen, and P. A. Lee, Phys. Rev. Lett. **66**, 3048 (1991).
[7] Y. Meir, N. S. Wingreen, and P. A. Lee, Phys. Rev. Lett. **70**, 2601 (1993).
[8] N. D. Lang, Phys. Rev. B **52**, 5335 (1995).
[9] F. Evers, F. Weigend, and M. Koentopp, Phys. Rev. B **69**, 235411 (2004).
[10] *A Primer in Density Functional Theory*, edited by C. Fiolhais, F. Nogueira, and M. Marques (Springer, New York, 2003).
[11] M. Koentopp, C. Chang, K. Burke, and R. Car, J. Phys. Condens. Matter **20**, 083203 (2008).
[12] W. Kohn and L. J. Sham, Phys. Rev. **140**, A1133 (1965).
[13] D. S. Fisher and P. A. Lee, Phys. Rev. B **23**, 6851 (1981).
[14] H. U. Baranger and A. D. Stone, Phys. Rev. B **40**, 8169 (1989).
[15] M. Koentopp, K. Burke, and F. Evers, Phys. Rev. B **73**, 121403 (2006).
[16] N. Sai, M. Zwolak, G. Vignale, and M. Di Ventra, Phys. Rev. Lett. **94**, 186810 (2005).
[17] J. Jung, P. Bokes, and R. W. Godby, Phys. Rev. Lett. **98**, 259701 (2007).
[18] J. P. Perdew, K. Burke, and M. Ernzerhof, Phys. Rev. Lett. **77**, 3865 (1996).
[19] A. D. Becke, J. Chem. Phys. **98**, 5648 (1993).
[20] J. P. Perdew, M. Ernzerhof, and K. Burke, J. Chem. Phys. **105**, 9982 (1996).
[21] J. P. Perdew and A. Zunger, Phys. Rev. B **23**, 5048 (1981).
[22] C. Toher, A. Filippetti, S. Sanvito, and K. Burke, Phys. Rev. Lett. **95**, 146402 (2005).
[23] D. J. Carrascal and J. Ferrer, Phys. Rev. B **85**, 045110 (2012).
[24] P. Schmitteckert and F. Evers, Phys. Rev. Lett. **100**, 086401 (2008).

[25]J. P. Bergfield, Z.-F. Liu, K. Burke, and C. A. Stafford, Phys. Rev. Lett. **108**, 066801 (2012).
[26]P. Tröster, P. Schmitteckert, and F. Evers, Phys. Rev. B **85**, 115409 (2012).
[27]G. Stefanucci and S. Kurth, Phys. Rev. Lett. **107**, 216401 (2011).
[28]P. W. Anderson, Phys. Rev. **124**, 41 (1961).
[29]J. P. Bergfield and C. A. Stafford, Phys. Rev. B **79**, 245125 (2009).
[30]J. P. Bergfield, G. Solomon, C. A. Stafford, and M. Ratner, Nano Lett. **11**, 2759 (2011).
[31]P. B. Wiegmann and A. M. Tsvelick, J. Phys. C **16**, 2281 (1983).
[32]J. Friedel, Nuovo Cimento Suppl. **7**, 287 (1958).
[33]D. C. Langreth, Phys. Rev. **150**, 516 (1966).
[34]H. Mera, K. Kaasbjerg, Y. M. Niquet, and G. Stefanucci, Phys. Rev. B **81**, 035110 (2010).
[35]J. P. Perdew, R. G. Parr, M. Levy, and J. L. Balduz, Phys. Rev. Lett. **49**, 1691 (1982).
[36]M. Pustilnik and L. Glazman, J. Phys. Condens. Matter **16**, R513 (2004).
[37]V. Zlatić and B. Horvatić, Phys. Rev. B **28**, 6904 (1983).
[38]S. Schmitt, T. Jabben, and N. Grewe, Phys. Rev. B **80**, 235130 (2009).
[39]In Refs. 48 and 49, this expansion was reported incorrectly, with the minus sign on the second term. We believe it corresponds to Wilson ratio $R = 1$; however, this is not true in the strongly correlated limit.
[40]K. Yosida and K. Yamada, Prog. Theor. Phys. Suppl. **46**, 244 (1970).
[41]K. Yamada, Prog. Theor. Phys. **53**, 970 (1975).
[42]K. Yosida and K. Yamada, Prog. Theor. Phys. **53**, 1286 (1975).
[43]N. A. Lima, M. F. Silva, L. N. Oliveira, and K. Capelle, Phys. Rev. Lett. **90**, 146402 (2003).
[44]S. Kurth, G. Stefanucci, E. Khosravi, C. Verdozzi, and E. K. U. Gross, Phys. Rev. Lett. **104**, 236801 (2010).
[45]V. I. Anisimov, J. Zaanen, and O. K. Andersen, Phys. Rev. B **44**, 943 (1991).
[46]H. J. Kulik, M. Cococcioni, D. A. Scherlis, and N. Marzari, Phys. Rev. Lett. **97**, 103001 (2006).
[47]J. P. Perdew, A. Savin, and K. Burke, Phys. Rev. A **51**, 4531 (1995).
[48]A. C. Hewson, *The Kondo Problem to Heavy Fermions* (Cambridge University Press, Cambridge, 1997).
[49]F. Evers and P. Schmitteckert, Phys. Chem. Chem. Phys. **13**, 14417 (2011).